Cell

Multiple Autism-Linked Genes Mediate Synapse Elimination via Proteasomal Degradation of a Synaptic Scaffold PSD-95

Nien-Pei Tsai,[1,4] Julia R. Wilkerson,[1,4] Weirui Guo,[1] Marina A. Maksimova,[1] George N. DeMartino,[2] Christopher W. Cowan,[3,5] and Kimberly M. Huber[1,*]
[1]Department of Neuroscience
[2]Department of Physiology
[3]Departments of Psychiatry and Ophthalmology
University of Texas Southwestern Medical Center, Dallas, TX 75390, USA
[4]These authors contributed equally to this work
[5]Present address: Department of Psychiatry, Harvard Medical School, McLean Hospital, Belmont, MA 02478, USA
*Correspondence: kimberly.huber@utsouthwestern.edu
http://dx.doi.org/10.1016/j.cell.2012.11.040

SUMMARY

The activity-dependent transcription factor myocyte enhancer factor 2 (MEF2) induces excitatory synapse elimination in mouse neurons, which requires fragile X mental retardation protein (FMRP), an RNA-binding protein implicated in human cognitive dysfunction and autism. We report here that protocadherin 10 (Pcdh10), an autism-spectrum disorders gene, is necessary for this process. MEF2 and FMRP cooperatively regulate the expression of Pcdh10. Upon MEF2 activation, PSD-95 is ubiquitinated by the ubiquitin E3 ligase murine double minute 2 (Mdm2) and then binds to Pcdh10, which links it to the proteasome for degradation. Blockade of the Pcdh10-proteasome interaction inhibits MEF2-induced PSD-95 degradation and synapse elimination. In FMRP-lacking neurons, elevated protein levels of eukaryotic translation elongation factor 1 α (EF1α), an Mdm2-interacting protein and FMRP target mRNA, sequester Mdm2 and prevent MEF2-induced PSD-95 ubiquitination and synapse elimination. Together, our findings reveal roles for multiple autism-linked genes in activity-dependent synapse elimination.

INTRODUCTION

Sensory experience, learning, and neuronal activity stabilize or eliminate select excitatory synapses and sculpt the mature neuronal circuits that mediate sensory processing and memory (Xu et al., 2009; Yang et al., 2009). The cellular mechanisms that underlie activity or experience-dependent synapse elimination in the central nervous system are largely unknown. The discovery that activation of the myocyte enhancer factor 2 (MEF2) family of transcription factors suppresses synapse number provides an important molecular link to understand how neuronal activity leads to synapse elimination (Flavell et al., 2006; Pfeiffer et al., 2010; Tian et al., 2010). MEF2 is activated upon neuronal depolarization and calcium influx, which induces the expression of MEF2 target genes that are thought to lead to synapse elimination (Flavell et al., 2006, 2008; McKinsey et al., 2002; Pulipparacharuvil et al., 2008). The identity of the MEF2 target genes that promote synapse elimination or their mechanisms of action in synapse elimination is unknown. We recently demonstrated that MEF2-induced synapse elimination requires fragile X mental retardation protein (FMRP) (Pfeiffer et al., 2010), an RNA-binding protein that regulates translation of its target mRNAs (Bassell and Warren, 2008). FMRP is encoded by the *Fmr1* gene, which is transcriptionally silenced in patients with fragile X syndrome (FXS), the most common inherited form of intellectual disability and autism (Abrahams and Geschwind, 2008; Kelleher and Bear, 2008). In neurons of the mouse model of FXS, *Fmr1* knockout (KO), MEF2-triggered synapse elimination is absent (Pfeiffer et al., 2010), which may contribute to the observed excess of dendritic spines on cortical neurons of FXS patients and the *Fmr1* KO mouse (Bagni and Greenough, 2005). The mechanisms that underlie the deficiencies in synapse elimination associated with FXS are unknown. Our previous results indicated that FMRP functions downstream of MEF2-induced transcription to eliminate synapses (Pfeiffer et al., 2010). Based on the known function of FMRP, we hypothesized that FMRP regulated translation of MEF2-generated transcripts.

To identify candidate transcripts involved in synapse elimination, we compared the known MEF2 target genes (Flavell et al., 2008) with FMRP-interacting mRNAs (Darnell et al., 2011). Of the many common MEF2- and FMRP-interacting transcripts, we focused on protocadherin 10 (*Pcdh10*), also known as OL-protocadherin, a member of the cadherin superfamily of calcium-dependent cell adhesion molecules (Morishita and Yagi, 2007). Importantly, homologous deletion of *Pcdh10* in humans is associated with autism (Morrow et al., 2008). Pcdh10 and other family members of the δ2 nonclustered protocadherin family (Pcdh8 and 19) demonstrate weak homophilic

binding activity relative to the classical cadherins (Hirano et al., 1999). Furthermore, the diverse structure of protocadherins' cytoplasmic C termini is consistent with the multifunctional roles of protocadherins in cell signaling and function, in addition to cell adhesion (Kim et al., 2011; Yasuda et al., 2007). *Pcdh10* is primarily expressed in the brain (Hirano et al., 1999), where it is required for the growth of striatal axons and patterning of thalamocortical and corticothalamic projections during embryonic development (Uemura et al., 2007). Interestingly, *Pcdh10* is highly expressed in mature cortical neurons, where nothing is known of its function (Kim et al., 2011).

Here, we demonstrate that Pcdh10 is required for MEF2-induced synapse elimination and functions to deliver ubiquitinated postsynaptic density protein 95 (PSD-95), a critical synaptic scaffolding molecule to the proteasome. *Fmr1* KO neurons have deficits in ubiquitination and degradation of PSD-95, and we uncover the molecular basis of this defect. Our results reveal mechanisms by which the activity-dependent transcription factor MEF2 refines synaptic connections in wild-type neurons and identify the mechanisms that underlie abnormal synapse refinement in fragile X syndrome. Importantly, this work demonstrates the necessity and distinct cellular functions of three genes linked to autism in the same synapse elimination process (*Pcdh10*, *Fmr1*. and *Mef2*; Novara et al., 2010) and thus provides evidence for a common synaptic deficit among different genetic causes of autism.

RESULTS

MEF2 and FMRP Regulate Pcdh10 Expression in Dendrites

To study the role of *Pcdh10* in MEF2 and FMRP regulation of synapse number, we first validated the association of FMRP and *Pcdh10* mRNA (Darnell et al., 2011). We performed an RNA immunoprecipitation with an anti-FMRP antibody and pulled down *Pcdh10* mRNA from hippocampal lysates of wild-type (WT) mice, but not *Fmr1* KO mice (Figure 1A), providing evidence for *Pcdh10* as an mRNA target of FMRP. We next examined whether *Pcdh10* expression is regulated by MEF2 and FMRP, using lentivirus to transfect tamoxifen-inducible, constitutively active MEF2 (MEF2-VP16ERtm) (Flavell et al., 2006; Pfeiffer et al., 2010) into dissociated cortical neuron cultures, which are amenable to biochemical assays. Basal levels of *Pcdh10* mRNA and another MEF2 target gene *Nurr77* were not different between WT and *Fmr1* KO neurons (vehicle; white bars, Figure 1B). After 6 hr of 4-hydroxytamoxifen (tamoxifen, 1 μm) treatment, which induces translocation of MEF2-VP16ERtm to the nucleus to activate target genes (Flavell et al., 2006), both *Pcdh10* and *Nurr77* mRNAs were elevated in WT and *Fmr1* KO neurons (black bars, Figure 1B), indicating that FMRP is not required for MEF2-induced transcription of target genes. Surprisingly, the level of *Pcdh10* mRNA induced with MEF2 activation in *Fmr1* KO neurons was greater than in WT neurons, perhaps reflecting a role of FMRP in RNA stability (Zhang et al., 2007). In contrast, Pcdh10 protein is basally higher in *Fmr1* KO neurons and is unresponsive to MEF2 activation (Figure 1C). Similar to cultured neurons, Pcdh10 protein is elevated in hippocampal lysates of *Fmr1* KO mice (Figures 1D and S1A). One function of FMRP is to suppress translation of its mRNA targets (Darnell et al., 2011; Napoli et al., 2008), suggesting that elevated Pcdh10 in *Fmr1* KO neurons is due to increased translation rate. To test this possibility, we performed metabolic labeling under basal and MEF2 activated conditions. ^{35}S-Met/Cys was added with vehicle or tamoxifen for 6 hr to MEF2-VP16ERtm-transfected cultures followed by immunoprecipitation of Pcdh10 or Tubulin (normalization control). We observed enhanced newly synthesized Pcdh10 in WT neurons upon tamoxifen treatment (Figure 1E). In *Fmr1* KO neurons, basal translation rates of Pcdh10 were elevated and MEF2 activation failed to further increase Pcdh10 synthesis. To determine whether MEF2 regulates the half-life of Pcdh10, we applied a 2 hr pulse of ^{35}S-Met/Cys label to neuronal cultures and chased this with fresh medium containing vehicle or tamoxifen for the time points indicated in Figure 1F. The half-life of Pcdh10 was not affected by genotype or MEF2 activation (Figure 1F). This data indicates that the elevated basal levels of Pcdh10 in *Fmr1* KO neurons are due to elevated protein synthesis rates and not reduced turnover.

To determine whether dendritic Pcdh10 protein levels are elevated in *Fmr1* KO neurons and to assess the cell autonomous role of FMRP in regulation of Pcdh10, we performed immunohistochemistry for Pcdh10 and microtubule-associated protein 2 (MAP2), a dendritic marker, in dissociated neuron cultures prepared from GFP/*Fmr1* mosaic mice (i.e., GFP+ cells are "wild type" and GFP− cells are *Fmr1* KO; see Extended Experimental Procedures available online). Immunohistochemistry confirmed that FMRP and GFP are coexpressed in hippocampal and cortical neurons of GFP/*Fmr1* mosaic mice (Niere et al., 2012) (Figure S1B). Pcdh10, but not MAP2, were elevated in both the soma and dendrites of *Fmr1* KO neurons (Figure 1G) in comparison to neighboring GFP+, WT neurons. These results support a role for FMRP in translational suppression of *Pcdh10*, which leads to elevated Pcdh10 in *Fmr1* KO neurons.

Immunohistochemistry for Pcdh10 in WT cultures revealed that Pcdh10 was present in dendritic spines where PSD-95, the postsynaptic excitatory synapse marker, was also enriched (Figure 1H). To validate the specificity of the antibody used for immunohistochemistry, we performed staining on hippocampal neurons transfected with two independent shRNAs against *Pcdh10* (Figure S1C). The results showed similar knockdown efficiency (>50%) by shRNAs as observed with western blot (Figures 3F and S3B), validating the fluorescence signal of Pcdh10 seen in Figure 1H. Therefore, Pcdh10 is present in spines at the site of excitatory synapses and may function in MEF2 regulation of excitatory synapse number.

Pcdh10 Is Required for MEF2-Induced Synapse Elimination

Because the expression of Pcdh10 is regulated by both MEF2 and FMRP, we hypothesized that Pcdh10 is required for MEF2- and FMRP-dependent synapse elimination (Pfeiffer et al., 2010). We first determined whether manipulation of Pcdh10 alone was sufficient to affect excitatory synaptic transmission. To do this, we overexpressed mouse Pcdh10 in WT organotypic hippocampal slice cultures using biolistic transfection (Figures S2A and S2B) (Pfeiffer et al., 2010). At 16–30 hr after

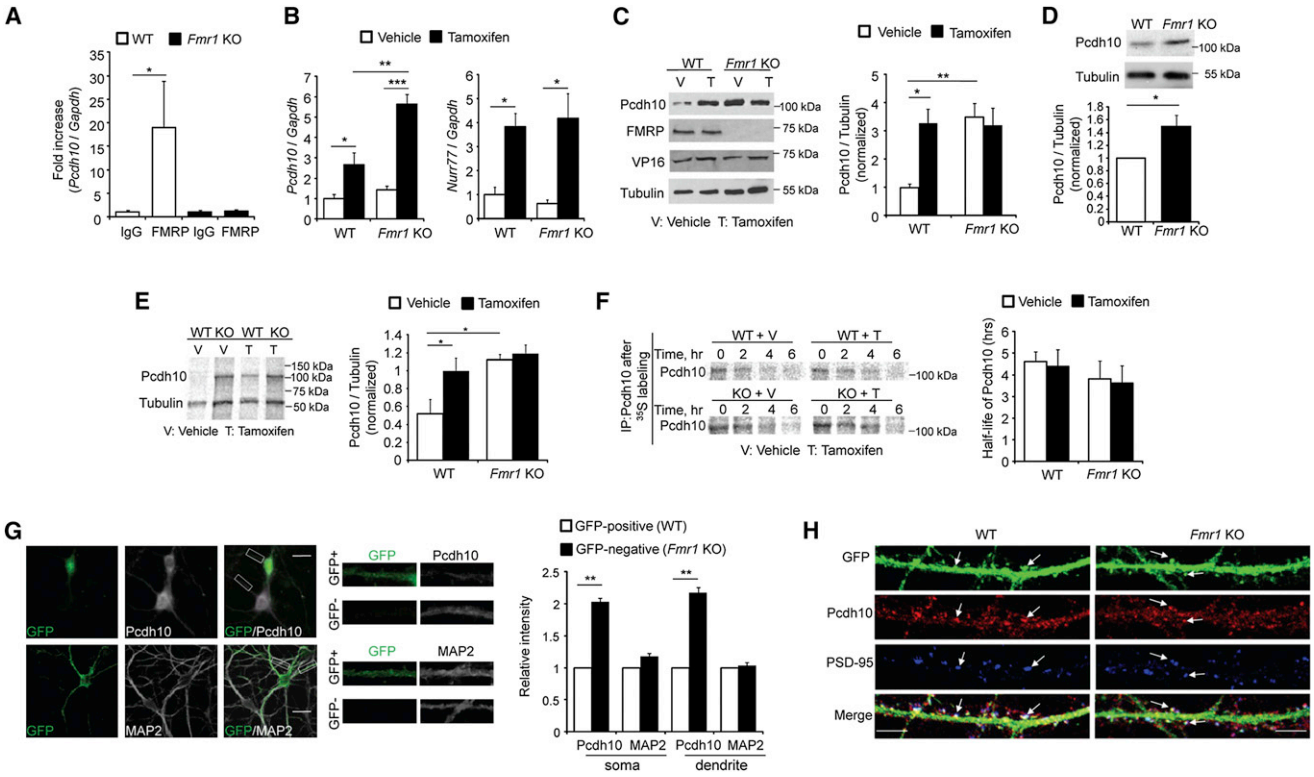

Figure 1. MEF2 and FMRP Coregulate Pcdh10 Expression

(A) Quantitative real-time RT-PCR of Pcdh10 precipitated with anti-FMRP antibody or IgG from wild-type (WT) or *Fmr1* KO mouse brains. Plotted is average of *Pcdh10*/*Gapdh* mRNA. n = 5 mice per genotype.

(B and C) (B) Quantitative real-time RT-PCR of *Pcdh10*/*Gapdh* and *Nurr77*/*Gapdh* mRNA and (C) Western blots of Pcdh10 from vehicle (V)- or 4-hydroxytamoxifen-treated (tamoxifen or "T") WT or *Fmr1* KO cortical neurons transfected with MEF2-VP16ERtm. n = 5 independent cultures for real-time RT-PCR and n = 3 for western blots.

(D) Western blots of Pcdh10 from WT or *Fmr1* KO hippocampi. n = 4 mice per genotype.

(E) ^{35}S-Met/Cys metabolic labeling from vehicle-treated or tamoxifen-treated (T) WT or *Fmr1* KO cortical neurons transfected with MEF2-VP16ERtm followed by immunoprecipitation of Pcdh10 and Tubulin. Plotted is average of Pcdh10/Tubulin. n = 3 cultures.

(F) ^{35}S-Met/Cys pulse-chase assay of Pcdh10 from vehicle- or T-treated WT or *Fmr1* KO cortical neurons transfected with MEF2-VP16ERtm. Plotted is average half-life of Pcdh10. n = 3 cultures.

(G) Immunohistochemistry of GFP with Pcdh10 or MAP2 from hippocampal neurons of GFP/*Fmr1* mosaic mouse. Selected GFP-positive (WT) and GFP-negative (*Fmr1* KO) areas are enlarged in the middle. Quantification of fluorescence intensity from soma and dendrites is shown on the right. Scale bar, 20 μm. n = 21 cells for both WT and *Fmr1* KO.

(H) Immunohistochemistry of Pcdh10 and PSD-95 from dissociated hippocampal neurons of WT or *Fmr1* KO mice.

GFP was used to visualize dendritic spines. Arrows indicate spines. Error bars represent SEM. Scale bar, 5 μm. *p < 0.05, **p < 0.01, ***p < 0.001. See also Figure S1.

transfection, we performed simultaneous whole-cell patch clamp recordings from Pcdh10-transfected and neighboring untransfected CA1 pyramidal neurons. Pcdh10 overexpression had no effect on excitatory synaptic transmission, as measured by the frequency or amplitude of miniature (m) EPSCs or evoked EPSC amplitude (Figure S2B and Table S1). Similarly, there was no effect of Pcdh10 on paired-pulse facilitation (PPF) of evoked EPSCs, an indicator of presynaptic release probability (Table S1). In the converse experiment, we knocked down endogenous Pcdh10 in WT hippocampal slice cultures using either one of two shRNAs targeting different regions of *Pcdh10* mRNA. After 40–60 hr transfection, neither shRNA against *Pcdh10* nor a control nontarget shRNA had any effect on the aforementioned measurements of excitatory synaptic function (Figures S2C, S2D, and S2E and Table S1). Similarly, transfection of dissociated hippocampal cultures with either Flag-Pcdh10 or shRNA against *Pcdh10* (Figures S2F and S2G) had no effect on synapse number, as measured by coclusters of the pre- and postsynaptic proteins synapsin-1 and PSD-95, or PSD-95 puncta number and size. These results indicate that acute changes in Pcdh10 levels are not sufficient to affect excitatory synaptic function.

To test whether Pcdh10 is required for MEF2-induced synapse elimination, we cotransfected WT hippocampal slice cultures with plasmids generating either one of two shRNAs against *Pcdh10* together with MEF2-VP16ERtm. Sister cultures were cotransfected with a control shRNA together with MEF2-VP16ERtm. After 24 hr, tamoxifen was applied to the slices to activate MEF2 for another 16–32 hr, followed by simultaneous

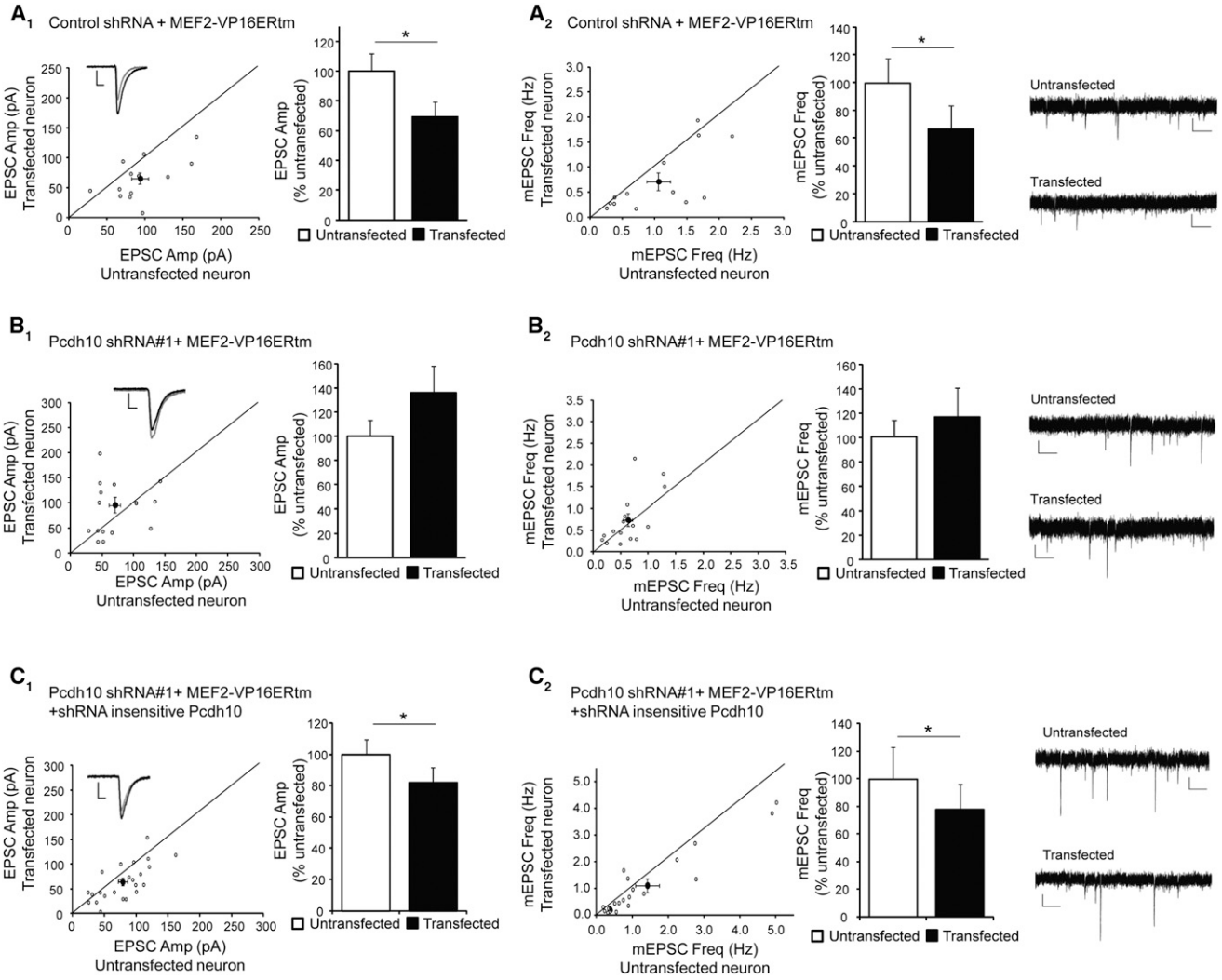

Figure 2. Pcdh10 Is Required for MEF2-Induced Functional Synapse Elimination in WT Neurons

(A) Average evoked EPSC amplitude (A_1) and mEPSC frequency (A_2) from untransfected and control shRNA with MEF2-VP16ERtm-transfected CA1 neurons in slice culture. n = 13 for both A_1 and A_2.

(B) Average evoked EPSC amplitude (B_1) and mEPSC frequency (B_2) from untransfected and Pcdh10 shRNA with MEF2-VP16ERtm-transfected cells. n = 16 for both B_1 and B_2.

(C) Average evoked EPSC amplitude (C_1) and mEPSC frequency (C_2) from untransfected and Pcdh10 shRNA with MEF2-VP16ERtm and shRNA-insensitive Pcdh10 construct-transfected cells. n = 24 for both C_1 and C_2.

Error bars represent SEM. *$p < 0.05$. Representative evoked EPSC and mEPSC traces are shown with the dot plots of individual cell pairs and on the right of each figure, respectively. See also Figure S2 and Table S1.

recordings of transfected and neighboring untransfected CA1 neurons. As shown, neurons transfected with MEF2-VP16ERtm and control shRNA had a decrease in mEPSC frequency and evoked EPSC amplitude but no change in PPF (Figure 2A and Table S1). These changes are consistent and correlate with structural synapse elimination that we previously demonstrated with MEF2-VP16ERtm in this preparation (Flavell et al., 2006; Pfeiffer et al., 2010). However, MEF2-induced functional synapse elimination was blocked in neurons transfected with shRNA against *Pcdh10* (Figures 2B and S2H and Table S1) and rescued by cotransfection of a shRNA-insensitive Pcdh10 (Figure 2C and Table S1) together with the *Pcdh10* shRNA. shRNA-mediated knockdown of *Pcdh10* did not affect MEF2-induced transcription of *Nurr77* as measured with real-time RT-PCR (Figure S2I), suggesting that *Pcdh10* functions in synapse elimination downstream of MEF2 activated transcription.

MEF2 Induces Pcdh10-Dependent Degradation of PSD-95

To determine the cellular mechanism by which Pcdh10 mediates MEF2-induced synapse elimination, we turned to dissociated cortical neuron cultures, which are amenable to biochemical methods. We hypothesized that MEF2 activation causes rapid

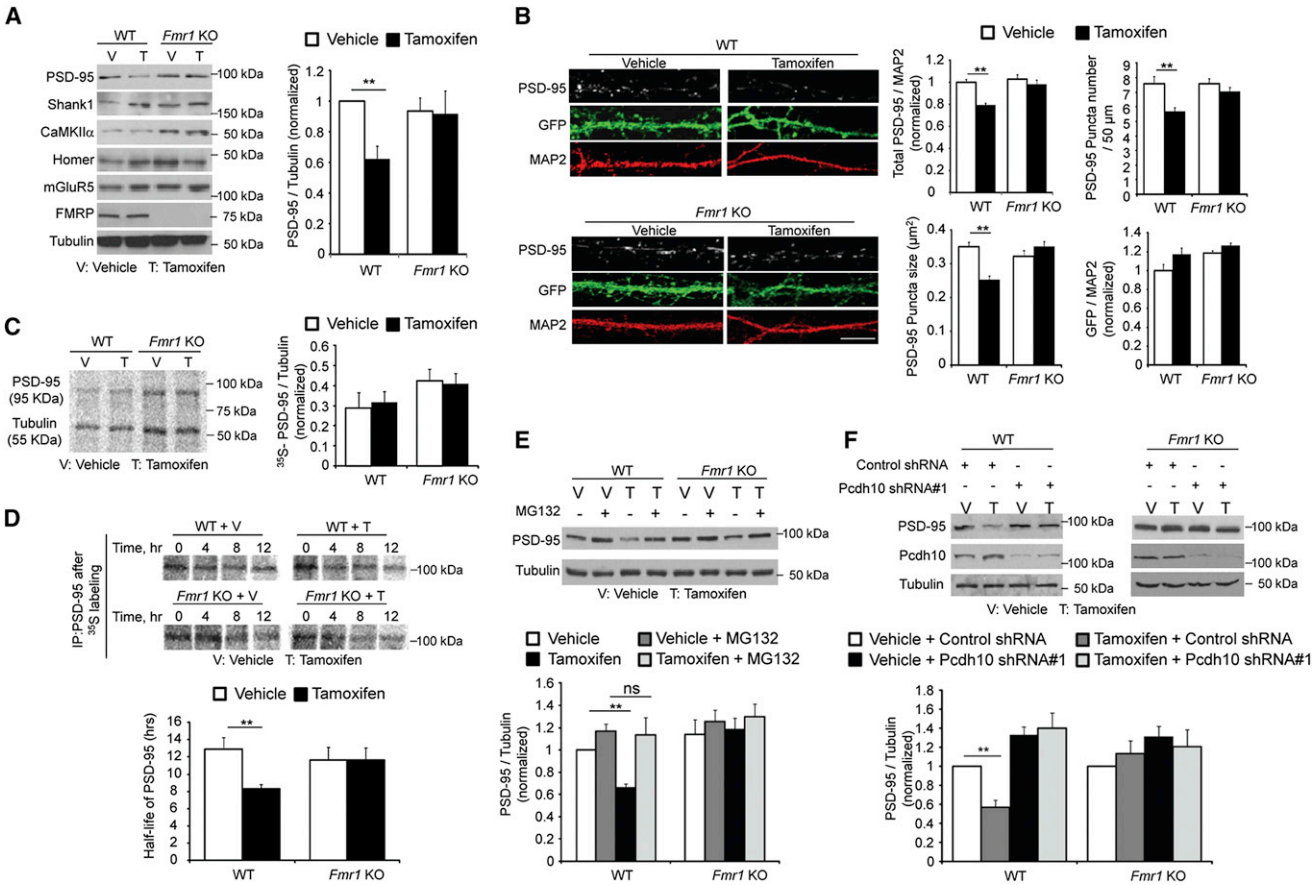

Figure 3. MEF2 Induces Pcdh10-Dependent Degradation of PSD-95

(A) Western blots of postsynaptic proteins from dissociated WT or *Fmr1* KO cortical neurons transfected with MEF2-VP16ERtm and treated with either vehicle or tamoxifen for 6 hr. Quantification of PSD-95 is shown on the right. n = 3 cultures.

(B) Immunohistochemistry of PSD-95 from dissociated WT or *Fmr1* KO hippocampal neurons transfected with MEF2-VP16ERtm and treated with either vehicle or tamoxifen for 6 hr. Bicistronic GFP from MEF2-VP16ERtm plasmid and endogenous MAP2 serve as transfection control and quantification control, respectively. Scale bars, 5 μm. Quantifications of total PSD-95 intensity, PSD-95 puncta number, PSD-95 puncta size, and GFP intensity are shown on the right. n = 21 cells/condition.

(C) ^{35}S-Met/Cys metabolic labeling from vehicle- or tamoxifen-treated WT or *Fmr1* KO cortical neurons transfected with MEF2-VP16ERtm followed by immunoprecipitation of PSD-95 and Tubulin. Plotted is average of Pcdh10/Tubulin. n = 3 cultures.

(D) ^{35}S-Met/Cys pulse-chase assay of Pcdh10 from vehicle- or tamoxifen-treated WT or *Fmr1* KO cortical neurons transfected with MEF2-VP16ERtm. Plotted is the average half-life of Pcdh10. n = 3 cultures.

(E) Western blots of PSD-95 and Tubulin from dissociated WT or *Fmr1* KO cortical neurons transfected with MEF2-VP16ERtm and treated with vehicle, tamoxifen, and/or proteasome inhibitor MG132, as indicated for 6 hr. Quantification is shown below. n = 4 cultures.

(F) Western blots of PSD-95, Pcdh10, and Tubulin from dissociated cortical neurons of WT or *Fmr1* KO mice transfected with MEF2-VP16ERtm and Pcdh10 shRNA. Quantification is shown below. n = 3 cultures.

Error bars represent SEM. **p < 0.01. See also Figure S3.

synapse elimination by the regulated degradation of synaptic scaffolding proteins. To investigate this possibility, we monitored the level of several postsynaptic scaffolding proteins in MEF2-VP16ERtm transfected cortical neuron cultures after 6 hr of tamoxifen treatment. As shown in Figure 3A, PSD-95 levels were significantly decreased in WT neurons, whereas other synaptic proteins (mGluR5, Homer, and CaMKIIα) remained unchanged. Consistent with the deficit in MEF2-induced synapse elimination in *Fmr1* KO neurons, PSD-95 levels were unchanged upon MEF2 activation in *Fmr1* KO neurons. Similar results were observed with immunohistochemistry for PSD-95 in dissociated hippocampal neurons (Figure 3B). This result also suggests that the downregulation of PSD-95 is a common consequence of MEF2 activation in both cortical and hippocampal neurons.

To determine whether the downregulation of PSD-95 resulted from reduced synthesis or increased degradation, we performed metabolic labeling with ^{35}S-Met/Cys in dissociated cortical neuron cultures. After 6 hr of MEF2 activation and ^{35}S-Met/Cys label, there was no change in newly synthesized PSD-95 from either WT or *Fmr1* KO neurons (Figure 3C). However, using the pulse-chase ^{35}S-Met/Cys labeling assay, the half-life of

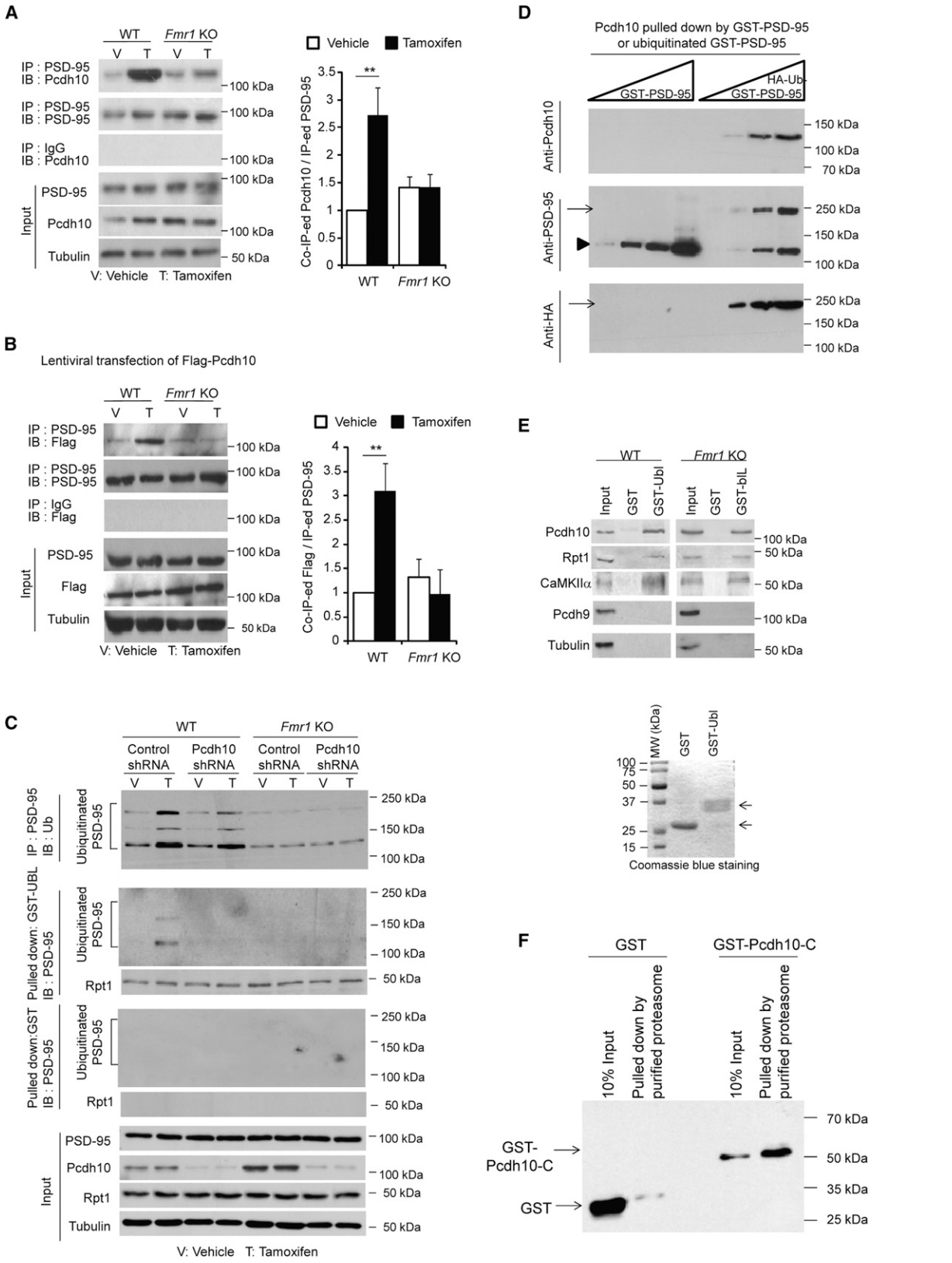

(legend continued on next page)

PSD-95 was reduced by ~35% after MEF2 activation in WT neurons (Figure 3D). Like PSD-95 protein levels (Figures 3A and 3B), PSD-95 half-life was unaffected by MEF2 activation in *Fmr1* KO neurons. To investigate whether MEF2-induced degradation of PSD-95 in WT neurons is proteasome dependent, we applied proteasome inhibitors MG132 (5 μM) or lactacystin (5 μM), together with tamoxifen (Figures 3E and S3A). Both MG132 and lactacystin blocked MEF2-induced downregulation of PSD-95 in WT neurons, and no changes in PSD-95 were observed under any condition in *Fmr1* KO neurons.

To determine whether MEF2-induced degradation of PSD-95 is mediated by Pcdh10, we used lentivirus to deliver MEF2-VP16ERtm along with one of two different shRNAs against *Pcdh10* into dissociated cortical neuron cultures. Knocking down *Pcdh10* with either shRNA inhibited MEF2-induced PSD-95 degradation (Figures 3F and S3B). PSD-95 degradation is rescued by lentiviral coexpression of shRNA-insensitive Pcdh10 together with the Pcdh10 shRNA (Figure S3C). These findings indicate that *Pcdh10* is required for MEF2-induced degradation of PSD-95 and suggest a molecular mechanism for *Pcdh10* in MEF2-induced synapse elimination.

Pcdh10 Facilitates the Proteasomal Deposition of Ubiquitinated PSD-95

To better determine the role of Pcdh10 in MEF2-induced regulation of PSD-95, we investigated whether Pcdh10 physically associated with PSD-95 and whether this changed with MEF2 activation. Using coimmunoprecipitation of Pcdh10 with PSD-95 from cortical neuron cultures (in the presence of MG132), we found that Pcdh10 could associate with PSD-95 (Figure 4A). Activation of MEF2 for 6 hr drastically increased the association between Pcdh10 and PSD-95 in WT neurons, but not in *Fmr1* KO neurons (Figure 4A). Similar results were obtained in hippocampal neuron cultures (Figure S4A). Given that MEF2 increases the expression of Pcdh10 in WT cultures (Figure 1D), we considered whether the MEF2-induced association of Pcdh10 and PSD-95 is due to enhanced production of Pcdh10. We used lentivirus to transfect WT or *Fmr1* KO cortical cultures with a Flag-tagged Pcdh10 driven by the cytomegalovirus (CMV) promoter whose transcription is not regulated by MEF2. Although total Flag-Pcdh10 levels were unchanged upon MEF2 activation, immunoprecipitation of PSD-95 revealed an increase in Flag-Pcdh10 association with PSD-95 (Figure 4B, in the presence of MG132). This suggests that MEF2 promotes the association of Pcdh10 with PSD-95 independent of regulating Pcdh10 levels. In *Fmr1* KO cultures, MEF2 activation did not stimulate an interaction of PSD-95 with Flag-Pcdh10, suggesting that the deficit in PSD95 degradation in *Fmr1* KO neurons is not due to the lack of MEF2-triggered Pcdh10 translation but instead on a distinct function of FMRP.

To determine the mechanism by which Pcdh10 regulates MEF2-dependent PSD-95 proteasomal degradation, we examined ubiquitination of PSD-95. MEF2 activation in WT cultures resulted in PSD-95 ubiquitination, as observed by immunoprecipitation of PSD-95 followed by western blotting with an anti-ubiquitin (Ub) antibody (in the presence of MG132, Figure 4C, top). Similar to previous reports (Colledge et al., 2003; Rezvani et al., 2007), polyubiquitinated PSD-95 was observed as multiple, distinct high-molecular-weight bands (115–200 kDa). Knockdown of Pcdh10 with a lentiviral-expressed shRNA had a slight effect on MEF2-induced PSD-95 ubiquitination. However, using GST-Ubl (ubiquitin-like domain from Rad23) (Bingol et al., 2010) to pull down the proteasome and proteasome-interacting proteins (in the presence of MG132), we could only detect ubiquitinated PSD-95 in neurons transfected with MEF2 plus control shRNA, but not Pcdh10 shRNA (Figure 4C, second panel from the top, and S4B). These results suggest that the predominant role of Pcdh10 is to associate ubiquitinated PSD-95 with the proteasome.

Because Pcdh10 is important for association of ubiquitinated PSD-95 with the proteasome, we next asked whether PSD-95 ubiquitination or proteasome association is deficient in *Fmr1* KO neurons. In contrast to WT cultures, MEF2 activation in *Fmr1* KO cultures failed to increase PSD-95 ubiquitination (Figure 4C). Consistent with these results, basal ubiquitination of PSD-95 is reduced in vivo in *Fmr1* KO hippocampi (Figure S4C). Taken together, these findings suggest that FMRP and Pcdh10 have distinct roles in MEF2-induced PSD-95 degradation: (1) FMRP is required for MEF2-induced ubiquitination of PSD-95, and (2) Pcdh10 is primarily required for linking ubiquitinated PSD-95 to the proteasomal machinery.

Based on results in WT cultures, we hypothesize that Pcdh10 associates ubiquitinated PSD-95 with the proteasome. To test this idea, we determined whether Pcdh10 interacts with ubiquitinated PSD-95 in vitro. We prepared native and ubiquitinated GST-PSD-95 by in vitro ubiquitination and observed that

Figure 4. Pcdh10 Facilitates the Proteasomal Degradation of Ubiquitinated PSD-95

(A and B) Western blots of (A) endogenous Pcdh10 or (B) Flag-Pcdh10 coimmunoprecipitated by anti-PSD-95 antibody. Protein samples were from dissociated WT or *Fmr1* KO cortical neurons transfected with (A) MEF2-VP16ERtm or (B) MEF2-VP16ERtm plus Flag-Pcdh10 and treated with either vehicle or tamoxifen for 6 hr. Inputs and quantification results are shown on the bottom and on the right. n = 4 cultures.

(C) Western blots of ubiquitin after immunoprecipitation of PSD-95 (top). Western blots of PSD-95 and Rpt1 after pull-down with GST-Ubl (second and third panels from the top). Western blots of PSD-95 and Rpt1 after pull-down with GST alone (fourth and fifth panels from the top). Protein samples were from dissociated WT or *Fmr1* KO cortical neurons transfected with MEF2-VP16ERtm with either control shRNA or Pcdh10 shRNA. Treatment is as indicated, and inputs are shown on the bottom.

(D) Western blots of Pcdh10 from WT brain lysates pulled down by increasing amount of native GST-PSD-95 or in vitro ubiquitinated GST-PSD-95. GST-PSD-95 used for the assay was detected by anti-PSD-95 antibody shown in the middle panel, whereas ubiquitinated GST-PSD-95 was detected by anti-HA antibody shown on the bottom. Arrowhead and arrows indicate native and ubiquitinated PSD-95, respectively.

(E) Western blots of Pcdh10, Rpt1, CaMKIIα, Pcdh9, and Tubulin from WT or *Fmr1* KO mice brains after pull-down with either GST or GST-Ubl. GST proteins used are shown on the bottom after Coomassie blue staining on a SDS-PAGE gel.

(F) Western blots of GST or GST-Pcdh10-C terminus pulled down by purified proteasome from Flag-Rpt6 stably expressing HEK293 cells.

Experiments in (A), (B), and (C) were done in the presence of MG132. Error bars represent SEM. **p < 0.01. See also Figure S4.

Pcdh10 from WT brain lysates preferentially interacts with ubiquitinated, but not native, GST-PSD-95 (Figure 4D). Ubiquitinated GST-PSD-95 failed to interact with in-vitro-translated Pcdh10 (Figure S4D), suggesting that posttranslational modifications of Pcdh10 or other interacting proteins are necessary. To test whether Pcdh10 interacts with the proteasome, we used GST-Ubl to pull down the proteasome and find that Pcdh10, the proteasome component Rpt1 (Demartino and Gillette, 2007), and the proteasome-interacting protein CaMKIIα (Bingol et al., 2010) were pulled down from both WT and *Fmr1* KO mouse brain (Figure 4E). In contrast, another protocadherin-δ family member, Pcdh9 (Morishita and Yagi, 2007), was not pulled down by GST-Ubl. The interaction of Pcdh10 and the proteasome was also confirmed by the demonstration that the GST-tagged C terminus of Pcdh10 interacts with a purified proteasome preparation from Flag-Rpt6 stably expressing HEK293 cells (Kim and DeMartino, 2011) (Figures 4F and S4E). Together, these results suggest that Pcdh10 interacts with ubiquitinated PSD-95 and the proteasome, and this interaction may not be conserved in other protocadherin family members.

We next determined whether MEF2-induced PSD-95 degradation and synapse elimination required Pcdh10 association with the proteasome. Toward this goal, we first mapped the minimum region of Pcdh10 that is required for interaction with the proteasome. We focused on the C terminus of Pcdh10 (266 amino acid) because it is predicted to be a cytoplasmic domain (Morishita and Yagi, 2007). We made various deletion constructs of the C terminus of Pcdh10 tagged with GST and tested their ability to pull down proteasomal complexes from brain lysates, as determined by association with the essential proteasome protein component Rpt1 (Bingol et al., 2010) (Figure 5A). Using this assay, we identified a 102 amino acid region (amino acids 778–879) of Pcdh10 required for the interaction with the proteasome. Amino acids 778–879 are highly conserved in Pcdh10 across species (Figure S5A), and we termed this sequence the proteasome interacting region (PIR).

We aimed to determine whether Pcdh10 association with the proteasome is necessary for MEF2-induced PSD-95 degradation and synapse elimination. In preparation for these experiments, we expressed a Flag-tagged PIR in WT cultured neurons and found that it distributes in dendrites and spines but did not alter general proteasome activity (Figures S5B and S5C). Importantly, Flag-PIR expression effectively competed with Pcdh10 and greatly reduced the association of endogenous Pcdh10 with the proteasome in neurons, as assessed by GST-Ubl pull-down (Figure 5B). Coexpression of Flag-PIR and MEF2-VP16ERtm in WT cortical neuron cultures blocked MEF2-induced degradation of PSD-95 (Figure 5C). Similarly, biolistic cotransfection of Flag-PIR and MEF2-VP16 into CA1 neurons of WT mouse hippocampal slice cultures blocked MEF2-induced functional synapse elimination (Figures 5D and 5E and Table S1) and MEF2-induced reduction in dendritic spine density (Figure 5F). Expression of Flag-PIR alone did not alter synaptic function (Figure S5D), spine density (Figure 5F), or MEF2-induced transcription (Figure S2I). These data demonstrate that Pcdh10 association with the proteasome is necessary for MEF2-induced PSD-95 degradation, as well as functional and structural synapse elimination. And based on these and our biochemical data (Figure 4), we propose that one role of Pcdh10 in synapse elimination is to deliver ubiquitinated PSD-95 to the proteasome for degradation.

The Ubiquitin E3 Ligase for PSD-95, Mdm2, Is Dysregulated in Fmr1 KO Neurons

In *Fmr1* KO neurons, MEF2-induced ubiquitination of PSD-95 is absent; a process that is independent of Pcdh10. To investigate the deficit in PSD-95 ubiquitination in *Fmr1* KO neurons, we examined the substrate-specific step of the ubiquitination process, which involves the ubiquitin E3 ligase for PSD-95, murine double minute 2 (Mdm2) (Colledge et al., 2003). Using shRNAs against Mdm2, we observed that Mdm2 is required for MEF2-induced PSD-95 ubiquitination (Figure 6A) and degradation (Figures 6B, S6A, S6B, and S6C) in WT cortical neurons, thus confirming that Mdm2 is the relevant E3 ligase for PSD-95. To investigate whether Mdm2 is dysregulated in *Fmr1* KO neurons, we performed coimmunoprecipitation and observed reduced interaction of Mdm2 and PSD-95 in *Fmr1* KO hippocampus in contrast to WT hippocampus (Figure 6C). Using immunohistochemistry for Mdm2 in dissociated hippocampal neurons, we also observed lower colocalization of Mdm2 with PSD-95 in dendrites of *Fmr1* KO neurons compared to WT neurons (Figure 6D). Although total Mdm2 levels were normal in *Fmr1* KO hippocampus (Figure 6C), Mdm2 levels in synaptoneurosome fractions of *Fmr1* KO hippocampi were reduced to about 40% of WT levels (Figure 6E). We hypothesized that MEF2 may enhance the synaptic localization of Mdm2, and this may be deficient in *Fmr1* KO neurons. To test this possibility, we activated MEF2 in dissociated cortical neuron cultures and examined Mdm2 levels in synaptoneurosome fractions and in coimmunoprecipitates with PSD-95. In WT neurons, MEF2 activation increased Mdm2 levels in synaptoneurosomes (Figure 6F), as well as the interaction between PSD-95 and Mdm2 (Figure 6G). In contrast, in *Fmr1* KO neurons, MEF2 failed to increase Mdm2 levels in synaptoneurosomes or the association of Mdm2 with PSD-95. MEF2 activation did not alter total Mdm2 levels in either WT or *Fmr1* KO cultures (Figures 6B and 6F). Together, these results indicate that MEF2 stimulates the localization of Mdm2 to the synaptic compartment and to PSD-95, and this process is defective in *Fmr1* KO neurons.

Elevated EF1α Inhibits Mdm2 from Interacting with PSD-95 in Fmr1 KO Neurons

In *Fmr1* KO neurons, Mdm2 localization at the synapse is reduced, and MEF2-induced redistribution of Mdm2 to synapses is deficient (Figure 6). We hypothesized that Mdm2 may have an abnormal interactome in *Fmr1* KO neurons. A previous proteomic study to identify human Mdm2 (Hdm2)-interacting proteins discovered a robust interaction of eukaryotic translation elongation factor 1-α (EF1α) and Hdm2 (Frum et al., 2007). EF1α is an FMRP target mRNA, and EF1α protein levels are upregulated in *Fmr1* KO brain (Darnell et al., 2011; Sung et al., 2003). We hypothesized that elevated EF1α in *Fmr1* KO neurons sequesters Mdm2 and prevents it from ubiquitinating PSD-95. In support of this hypothesis, immunoprecipitation of Mdm2 from hippocampal lysates revealed an increased interaction of EF1α and Mdm2 in vivo in *Fmr1* KO mice (Figure 7A). This increased

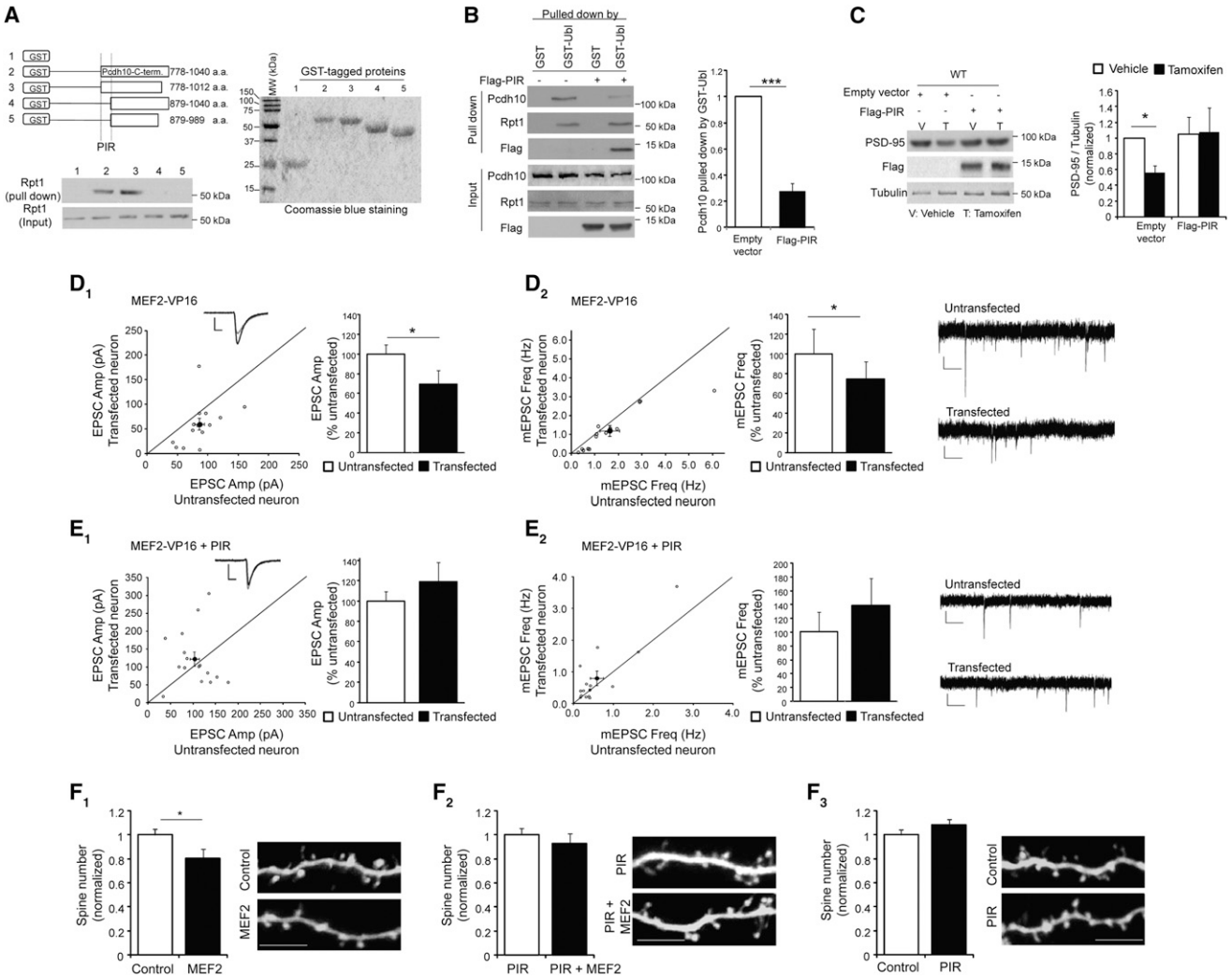

Figure 5. Blocking Interaction of Pcdh10 and Proteasome Inhibits MEF2-Induced PSD-95 Degradation and Synapse Elimination

(A) Western blots of Rpt1 from WT mouse brain after pull-down by GST alone or different GST-Pcdh10 carboxyl terminus proteins. Schematic diagram of Pcdh10-C-terminal deletions are shown on top. GST proteins used are shown on the right with Coomassie blue staining on a SDS-PAGE gel.

(B) Western blots of Pcdh10, Rpt1, and Flag from dissociated WT cortical neurons transfected with Flag-PIR after pull-down with either GST or GST-Ubl. Input of each protein and quantification are shown on the bottom and right, respectively. n = 3 cultures.

(C) Western blots of PSD-95, Flag, and Tubulin from dissociated WT cortical neurons transfected with MEF2-VP16ERtm and Flag-PIR with vehicle or tamoxifen treatment as indicated. Quantification of PSD-95 level is shown on the right. n = 4 cultures.

(D and E) Average evoked EPSC amplitude (D_1) and mEPSC frequency (D_2) from untransfected and control vector plus MEF2-VP16-transfected cells. n = 14 for both D_1 and D_2. (E) Average evoked EPSC amplitude (E_1) and mEPSC frequency (E_2) from untransfected and PIR plus MEF2-VP16-transfected cells. n = 16 for both E_1 and E_2. Representative evoked EPSC and mEPSC traces are shown with the dot plots and on the right of each figure, respectively.

(F) Quantification and representative images of apical secondary dendrites from WT CA1 pyramidal neurons transfected with GFP plus other plasmids as indicated. n = 10–20 cells in each condition. Scale bar, 5 μm.

Error bars represent SEM. *p < 0.05, ***p < 0.001. See also Figure S5 and Table S1.

interaction may be due to the observed increase in total EF1α protein in *Fmr1* KO (Figure 7A). To determine whether EF1α and PSD-95 directly compete for interactions with Mdm2, we obtained recombinant His-Mdm2, GST-EF1α, and GST-PSD-95. To Ni beads with bound His-Mdm2, we first added increasing amounts of GST-EF1α. After washing off unbound GST-EF1α, we incubated the complex with GST-PSD-95. Because a possible degraded product of His-Mdm2 runs at the same position of GST- EF1α on a SDS-PAGE, we used western blotting to detect the composition of the complex. As shown (Figure 7B), the binding of Mdm2 to EF1α occurs with a stoichiometry of ~1:1, and EF1α-bound Mdm2 lost the ability to bind PSD-95. His-Mdm2 also runs at a position approximately doubled to its predicted molecular weight, suggesting formation of homodimer (Dolezelova et al., 2012). The GST tag does not interact with His-Mdm2 nor interfere with the binding of His-Mdm2 to GST-EF1α or GST-PSD-95 (Figure S7A). To test the affinity of Mdm2 toward binding EF1α or PSD-95, we premixed GST- EF1α (1 pmol) and

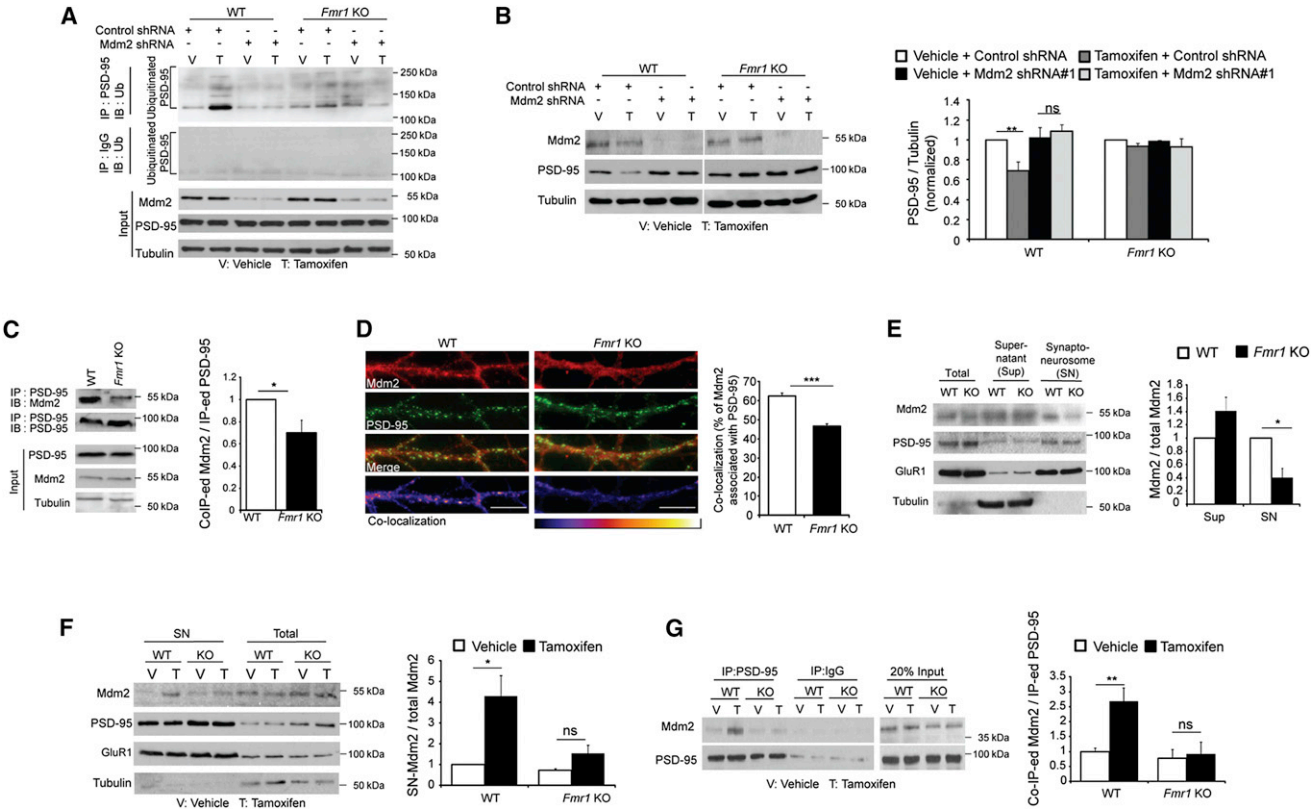

Figure 6. Mdm2 and Mdm2-Mediated Degradation of PSD-95 Are Dysregulated in *Fmr1* KO Neurons

(A) Western blots of ubiquitin after immunoprecipitation with PSD-95 (top) or IgG (second panel from the top). Protein samples were from dissociated WT or *Fmr1* KO cortical neurons transfected with either control shRNA or Mdm2 shRNA together with MEF2-VP16ERtm. Treatment was as indicated, and input was shown on the bottom.

(B) Western blots of PSD-95, Mdm2, and Tubulin from dissociated WT or *Fmr1* KO cortical neurons transfected with either control shRNA or Mdm2 shRNA together with MEF2-VP16ERtm. Quantification is shown on the right. n = 3 cultures.

(C) Western blots of Mdm2 immunoprecipitated with PSD-95 from WT or *Fmr1* KO hippocampi. n = 4 mice per genotype.

(D) Immunohistochemistry of dendritic Mdm2 with PSD-95 from dissociated WT or *Fmr1* KO hippocampal neurons. Colocalization images are shown on the bottom. Scale bars, 5 μm. Quantification of colocalization is shown on the right. n = 21 cells.

(E) Western blots of Mdm2, PSD-95, GluR1 (GluA1), and Tubulin in synaptoneurosomes prepared from WT or *Fmr1* KO hippocampi. Quantification of Mdm2 in supernatant or synaptoneurosome is shown on the right. n = 4 mice per genotype.

(F) Western blots of Mdm2, PSD-95, GluR1 (GluA1), and Tubulin after synaptoneurosome preparation of dissociated WT or *Fmr1* KO cortical neurons transfected with MEF2-VP16ERTm. Quantification of Mdm2 in synaptoneurosome is shown on the right. n = 3 cultures.

(G) Western blots of Mdm2 immunoprecipitated with PSD-95 from dissociated WT or *Fmr1* KO cortical neurons transfected with MEF2-VP16ERtm. Quantification is shown on the right. n = 3 cultures.

Error bars represent SEM. *p < 0.05, **p < 0.01, ***p < 0.001. Experiments in (A), (F), and (G) were done in the presence of MG132. See also Figure S6.

GST-PSD-95 (1 pmol), followed by adding Ni beads with bound His-Mdm2 (0.5 pmol). As shown in Figure 7C, Mdm2 has higher affinity toward binding EF1α over PSD-95. Together, these results indicate that EF1α can effectively compete with PSD-95 for binding to Mdm2.

We hypothesized that reducing EF1α levels in *Fmr1* KO neurons may release Mdm2, allow interactions with PSD-95, and rescue MEF2-induced PSD-95 degradation. To test this possibility, we applied a lentivirus expressing a shRNA against EF1α that reduced EF1α in *Fmr1* KO neurons to WT levels but did not affect Pcdh10 protein levels (Figure S7B). Knocking down EF1α in *Fmr1* KO neurons did not affect MEF2 activation (Figure S7C) but restored MEF2-induced synaptic localization of Mdm2 (Figure 7D) and the interaction between Mdm2 and PSD-95 (Figure 7E). Knocking down EF1α also restored MEF2-induced PSD-95 degradation in *Fmr1* KO neurons, which required Mdm2 (Figures 7F and S7D). Coexpression of a shRNA-insensitive EF1α together with the EF1α shRNA inhibited MEF2-induced synaptic accumulation of Mdm2 (Figure S7E), the interaction between PSD-95 and Mdm2 (Figure S7F), and PSD-95 degradation (Figure S7G) in *Fmr1* KO neurons, demonstrating the specificity of the EF1α shRNA. These results demonstrate that elevated EF1α in *Fmr1* KO neurons inhibits Mdm2 from interacting with PSD-95 and blocks the subsequent degradation of PSD-95.

To determine whether knocking down EF1α in *Fmr1* KO neurons could also restore MEF2-induced synapse elimination, we biolistically transfected *Fmr1* KO hippocampal slice cultures with a plasmid encoding a shRNA for EF1α or a control shRNA.

Expression of either shRNA alone had no effect on synaptic function (Figures S7H and S7I and Table S1). We then cotransfected *Fmr1* KO slice cultures with either control shRNA or EF1α shRNA together with MEF2-VP16ERtm and subsequently treated the cultures with tamoxifen. *Fmr1* KO neurons transfected with control shRNA had a deficit in MEF2-induced functional synapse elimination (Figure 7G), consistent with our previous report (Pfeiffer et al., 2010). As observed with PSD-95 degradation, EF1α shRNA transfection rescued robust functional synapse elimination in response to MEF2 activation (Figure 7H). Again, coexpression of a shRNA-insensitive EF1α together with the EF1α shRNA blocked MEF2-induced functional synapse elimination (Figure 7I). The shRNA-insensitive EF1α on its own did not affect excitatory synaptic function (Figure S7J). Taken together, our results indicate that elevated EF1α in *Fmr1* KO neurons inhibits Mdm2 from triggering PSD-95 degradation and subsequent synapse elimination by MEF2 in the *Fmr1* KO neurons. By knocking down EF1α, we were able to rescue the following in response to MEF2 activation: (1) synaptic redistribution of Mdm2, (2) the interaction between Mdm2 and PSD-95, (3) PSD-95 degradation, and (4) synapse elimination.

DISCUSSION

MEF2 Triggers Synapse Elimination by Promoting Pcdh10-Dependent Degradation of a Synaptic Scaffolding Protein

Here we identified a mechanism by which the activity-dependent transcription factor, MEF2, promotes synapse elimination as well as the molecular basis of the deficit in synapse elimination observed in fragile X syndrome, a prevalent cognitive and autistic disorder. In wild-type neurons, MEF2 activation induces transcription of *Pcdh10*, which mediates degradation of the synaptic scaffold PSD-95, and synapse elimination by associating ubiquitinated PSD-95 with the proteasome (Figure 7J). Although translation of *Pcdh10*, an FMRP target mRNA, is dysregulated in *Fmr1* KO neurons, we find a deficit in MEF2-stimulated ubiquitination of PSD-95, a step that is upstream and independent of *Pcdh10*. The deficit in PSD-95 ubiquitination in *Fmr1* KO neurons is caused by elevated levels of EF1α protein, an FMRP target mRNA, which sequesters Mdm2 from the synapse and PSD-95 (Figure 7J). In support of this conclusion, knockdown of EF1α levels rescues MEF2-induced PSD-95 degradation and synapse elimination in *Fmr1* KO neurons. Whether MEF2 regulates the interaction of EF1α and Mdm2 to regulate PSD-95 degradation in WT neurons is unknown.

Protocadherins and Synapse Elimination

The protocadherins are ancestors of the classical cadherins, the more well-known members of the Ca^{2+}-dependent cell adhesion molecule family (Giagtzoglou et al., 2009). Although the extracellular domains of protocadherins share homology with the traditional cadherins, they lack a hydrophobic pocket within extracellular domain 1 that is important for strong homophilic adhesion (Morishita et al., 2006; Morishita and Yagi, 2007). Consistent with this prediction, Pcdh10, when expressed in cell lines, clusters at points of cell contact and stimulates cell aggregation but less robustly than classical cadherins (Hirano et al., 1999). A recent study demonstrated that another δ2 nonclustered protocadherin family member, Pcdh8 or Arcadlin, is induced in neurons in response to seizures and interacts in *cis* with N-cadherin (a classical cadherin) in postsynaptic membranes. Homophilic interactions of Pcdh8, in *cis* or *trans*, recruit p38 MAPK to its C terminus, which in turn, stimulates the coendocytosis of Pcdh8 and N-cadherin and decreases dendritic spine density (Yasuda et al., 2007). An interesting possibility is that the induction of the δ2 Pcdhs, such as Pcdh8 and Pcdh10, functions to increase the membrane concentration and probability of homophilic Pcdh interactions, which activates key signaling pathways and their endocytosis. Such endocytosis could facilitate interactions of Pcdh10 with ubiquitinated PSD-95 and the proteasome.

MEF2 Promotes Degradation of a Postsynaptic Scaffold to Eliminate Synapses

MEF2 activation is associated with a rapid reduction of synapse number, suggesting that MEF2 eliminates pre-existing synapses (Flavell et al., 2006; Pfeiffer et al., 2010). However, MEF2 may also inhibit synapse formation rates. In support of an elimination mechanism, MEF2 activation caused a rapid and selective degradation of PSD-95 and a decrease in functional synapse number—effects that both required the MEF2 transcript, *Pcdh10*. Disrupting the association of Pcdh10 with the proteasome using the PIR peptide blocked MEF2-induced PSD-95 degradation, as well as functional and structural synapse elimination, suggesting that ubiquitination and Pcdh10-dependent degradation of PSD-95 are key steps that couple MEF2-driven transcription to synapse elimination. PSD-95 stabilizes synaptic AMPARs, increases synaptic function, and results in larger and more stable spines (Keith and El-Husseini, 2008; Opazo et al., 2011). Conversely, reductions in PSD-95 can lead to diffusion and endocytosis of synaptic AMPARs, weaker synapses, smaller spines, and spine elimination (Colledge et al., 2003; Haas et al., 2007; Keith and El-Husseini, 2008; Opazo et al., 2011; Woods et al., 2011). Specifically, in response to NMDAR activation, PSD-95 is ubiquitinated by Mdm2, degraded by the proteasome, removed from spines, and required for endocytosis of AMPARs (Colledge et al., 2003; Sturgill et al., 2009). Therefore, MEF2-triggered degradation of PSD-95 may cause destabilization and removal of synaptic AMPARs that precedes elimination of the structural synapse. Of note, knockdown of Pcdh10 prevented MEF2-induced functional synapse elimination, but not ubiquitination of PSD-95. This suggests that ubiquitination of PSD-95 is not sufficient to mediate functional synapse elimination, as Pcdh10-dependent targeting of ubiquitinated PSD-95 to the proteasome is also required.

Recapitulating Synapse Elimination in Fragile X Syndrome

Fragile X syndrome patients and *Fmr1 KO mice* display elevated dendritic spine number in mature cortical neurons, which may contribute to the neuronal hyperexcitability, sensory hypersensitivity, and epileptic seizures observed in patients and the mouse model (Berry-Kravis, 2002; Dölen et al., 2010). A deficit in activity and MEF2-dependent synapse elimination could lead to excess spines. In support of this idea, experience-dependent spine

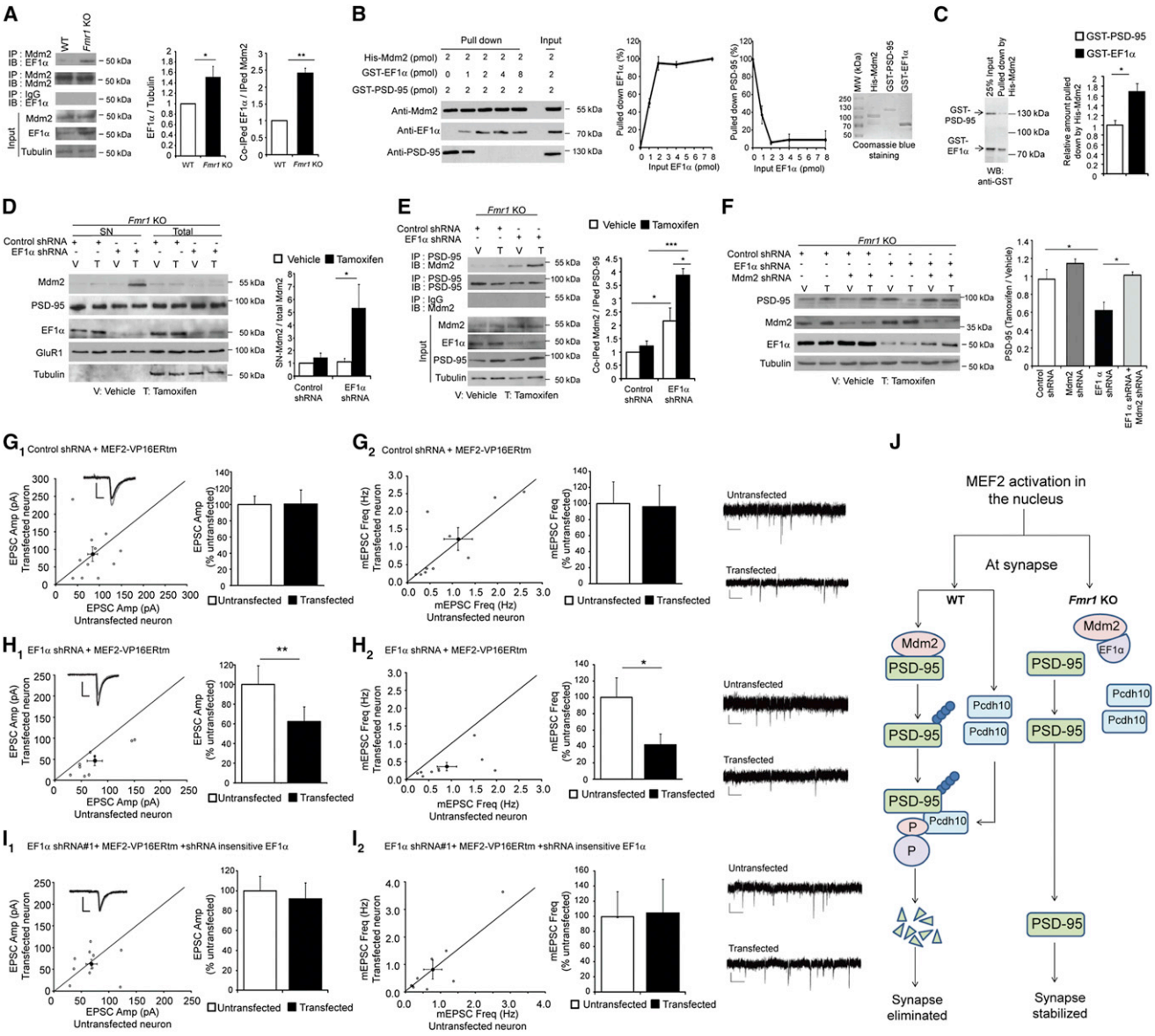

Figure 7. Elevated EF1α in *Fmr1* KO Neurons Inhibits Mdm2 from Interacting with PSD-95 and Subsequent PSD-95 Degradation

(A) Western blots of EF1α from WT or *Fmr1* KO hippocampi after immunoprecipitation by anti-Mdm2 antibody or IgG. Quantifications on total and immunoprecipitated EF1α with Mdm2 are shown on the right. n = 3 mice per genotype.

(B) Western blots of Mdm2, EF1α, and PSD-95 after in vitro sequential binding with recombinant proteins. Quantifications of binding and competition are shown in the middle (n = 3), whereas the purity of recombinant proteins is shown on the right with Coomassie-blue-stained SDS-PAGE gel.

(C) Western blots of GST- EF1α and GST-PSD-95 after in vitro binding with His-Mdm2. Quantification of relative amount of GST proteins pulled down by His-Mdm2 is on the right. n = 4.

(D) Western blots of Mdm2, PSD-95, EF1α, GluR1 (GluA1), and Tubulin after synaptoneurosome preparation of dissociated *Fmr1* KO cortical neurons transfected with MEF2-VP16ERtm and either control shRNA or EF1α shRNA. Quantification of Mdm2 in synaptoneurosome is shown on the right. n = 3 cultures.

(E) Western blots of Mdm2 immunoprecipitated with PSD-95 from dissociated *Fmr1* KO cortical neurons transfected with MEF2-VP16ERtm and either control shRNA or EF1α shRNA. Quantification is shown on the right. n = 3 cultures. Experiments in (D) and (E) were done in the presence of MG132.

(F) Western blots of PSD-95, Mdm2, EF1α, and Tubulin from dissociated *Fmr1* KO cortical neurons transfected with MEF2-VP16ERtm and either control shRNA, EF1α shRNA, and/or Mdm2 shRNA as indicated. Treatment with vehicle or tamoxifen is also as indicated. Quantification is shown on the bottom. n = 4 cultures.

(G) Average evoked EPSC amplitude (G_1) and mEPSC frequency (G_2) from untransfected and control shRNA with MEF2-VP16ERtm-transfected *Fmr1* KO cells. n = 11 for both G_1 and G_2.

(H) Average evoked EPSC amplitude (H_1) and mEPSC frequency (H_2) from untransfected and EF1α shRNA with MEF2-VP16ERtm-transfected *Fmr1* KO cells. n = 9 for both H_1 and H_2.

(legend continued on next page)

elimination in the somatosensory barrel cortex is deficient in *Fmr1* KO mice (Pan et al., 2010). The molecular mechanisms that lead to elevated dendritic spine number or the deficits in synapse elimination associated with fragile X are unknown. Current evidence suggests that FMRP functions as a translational switch of its target mRNAs. At steady state, FMRP suppresses translation of its mRNA targets in dendrites, and it derepresses or stimulates their translation upon synaptic stimulation dephosphorylation and/or degradation (Bassell and Warren, 2008; Niere et al., 2012). Consistent with this model, we observed elevated Pcdh10 translation rates in *Fmr1* KO neurons that were not stimulated by MEF2 despite induction of *Pcdh10* mRNA. Alternatively, Pcdh10 translation rates in *Fmr1* KO neurons may be saturated and cannot be further increased by elevated mRNA. We would expect that translational control of other FMRP target mRNAs that are induced in response to MEF2 would be similarly affected in *Fmr1* KO neurons.

Although translational control of Pcdh10 is abnormal in *Fmr1* KO neurons, our results suggest that this does not underlie the deficit in MEF2-induced synapse elimination. Knocking down EF1α restores MEF2-induced synapse elimination in *Fmr1 KO* mice without affecting Pcdh10 protein levels. Therefore, one requirement of FMRP in MEF2-induced synapse elimination is to suppress steady-state translation of EF1α and allow appropriate MEF2-regulated synaptic targeting of Mdm2 and PSD-95 ubiquitination. This highlights the importance of translational suppression and regulation of protein concentration in dendrites for proper synaptic plasticity. Loss-of-function mutations in the MEF2 isoform, *Mef2C*, *Fmr1*, or *Pcdh10* are all associated with autism, with or without intellectual disability (Abrahams and Geschwind, 2008; Morrow et al., 2008; Novara et al., 2010). Here, we have described distinct roles for all three genes in regulated degradation of PSD-95 and synapse elimination. This work suggests a common deficit in activity-dependent synapse elimination among different genetic causes of autism.

EXPERIMENTAL PROCEDURES

Organotypic Slice Culture and Dissociated Neuron Culture

Organotypic hippocampal slice cultures were made from postnatal day (P) 6–7 WT or *Fmr1* KO mice bred from the congenic C57BL/6 mouse strain and transfected as described (Pfeiffer et al., 2010) (Extended Experimental Procedures). Dissociated hippocampal or cortical cultures were prepared from P0-1 WT and *Fmr1* KO mice as described (Niere et al., 2012).

Electrophysiology

Dual whole-cell patch recordings were obtained from CA1 pyramidal neurons in slice cultures using IR-DIC and GFP fluorescence to identify nontransfected and transfected neurons as described (Pfeiffer et al., 2010) (Extended Experimental Procedures).

Synaptoneurosome Preparation

Hippocampal synaptoneurosomes were prepared as previously described (Waung et al., 2008). For synaptoneurosomes of dissociated cultures, cells were scraped off in buffer: 118 mM NaCl, 4.7 mM KCl, 1.2 mM $MgSO_4$, 2.5 mM $CaCl_2$, 1.53 mM KH_2PO_4, 212.7 mM glucose, 1 mM DTT (pH 7.4), and protease inhibitor cocktail (Calbiochem) followed by same procedures as described (Waung et al., 2008).

Statistical Analysis

For multiple comparisons, two-way ANOVA and Bonferroni posthoc tests were performed. Paired t tests were used for electrophysiology assays. Independent t test was used for Figures 1D, 5B, 5F, 6C, and 7A. In all figures, error bars represent SEM; *$p < 0.05$, **$p < 0.01$, ***$p < 0.001$.

SUPPLEMENTAL INFORMATION

Supplemental Information includes Extended Experimental Procedures, seven figures, and one table and can be found with this article at http://dx.doi.org/10.1016/j.cell.2012.11.040.

ACKNOWLEDGMENTS

This research was supported by grants from the National Institutes of Health NS045711, HD052731 (K.M.H.), F32HD069111 (N.-P.T.), F32HD062120 (J.R.W.) and from the Simons Foundations (K.M.H. and C.W.C.). We would also like to thank L. Ormazabal, N. Cabalo, F. Niere, K. Loerwald, T. Zang, D. Thompson, X. Li, and B. Chen for technical assistance; Dr. M. Rosen for the GST-*Pcdh10* constructs; Dr. J. Gibson for helpful discussions; and Drs. Robert and Jennifer Darnell for sharing their FMRP-CLIP target list prior to publication.

Received: February 25, 2012
Revised: August 29, 2012
Accepted: November 20, 2012
Published: December 20, 2012

REFERENCES

Abrahams, B.S., and Geschwind, D.H. (2008). Advances in autism genetics: on the threshold of a new neurobiology. Nat. Rev. Genet. *9*, 341–355.

Bagni, C., and Greenough, W.T. (2005). From mRNP trafficking to spine dysmorphogenesis: the roots of fragile X syndrome. Nat. Rev. Neurosci. *6*, 376–387.

Bassell, G.J., and Warren, S.T. (2008). Fragile X syndrome: loss of local mRNA regulation alters synaptic development and function. Neuron *60*, 201–214.

Berry-Kravis, E. (2002). Epilepsy in fragile X syndrome. Dev. Med. Child Neurol. *44*, 724–728.

Bingol, B., Wang, C.F., Arnott, D., Cheng, D., Peng, J., and Sheng, M. (2010). Autophosphorylated CaMKIIalpha acts as a scaffold to recruit proteasomes to dendritic spines. Cell *140*, 567–578.

Colledge, M., Snyder, E.M., Crozier, R.A., Soderling, J.A., Jin, Y., Langeberg, L.K., Lu, H., Bear, M.F., and Scott, J.D. (2003). Ubiquitination regulates PSD-95 degradation and AMPA receptor surface expression. Neuron *40*, 595–607.

Darnell, J.C., Van Driesche, S.J., Zhang, C., Hung, K.Y., Mele, A., Fraser, C.E., Stone, E.F., Chen, C., Fak, J.J., Chi, S.W., et al. (2011). FMRP stalls ribosomal translocation on mRNAs linked to synaptic function and autism. Cell *146*, 247–261.

Demartino, G.N., and Gillette, T.G. (2007). Proteasomes: machines for all reasons. Cell *129*, 659–662.

Dölen, G., Carpenter, R.L., Ocain, T.D., and Bear, M.F. (2010). Mechanism-based approaches to treating fragile X. Pharmacol. Ther. *127*, 78–93.

(I) Average evoked EPSC amplitude (I_1) and mEPSC frequency (I_2) from untransfected and EF1α shRNA with MEF2-VP16ERtm and shRNA-insensitive EF1α-transfected *Fmr1* KO cells (n = 13 for both I_1 and I_2). Error bars represent SEM. Representative evoked EPSC and mEPSC traces are shown with the dot plots and on the right of each figure, respectively. *$p < 0.05$, **$p < 0.01$.

(J) Working model of MEF2-induced synapse elimination in WT neurons and the molecular basis of the deficit in synapse elimination in *Fmr1* KO neurons. See also Figure S7 and Table S1.

Dolezelova, P., Cetkovska, K., Vousden, K.H., and Uldrijan, S. (2012). Mutational analysis of Mdm2 C-terminal tail suggests an evolutionarily conserved role of its length in Mdm2 activity toward p53 and indicates structural differences between Mdm2 homodimers and Mdm2/MdmX heterodimers. Cell Cycle *11*, 953–962.

Flavell, S.W., Cowan, C.W., Kim, T.K., Greer, P.L., Lin, Y., Paradis, S., Griffith, E.C., Hu, L.S., Chen, C., and Greenberg, M.E. (2006). Activity-dependent regulation of MEF2 transcription factors suppresses excitatory synapse number. Science *311*, 1008–1012.

Flavell, S.W., Kim, T.K., Gray, J.M., Harmin, D.A., Hemberg, M., Hong, E.J., Markenscoff-Papadimitriou, E., Bear, D.M., and Greenberg, M.E. (2008). Genome-wide analysis of MEF2 transcriptional program reveals synaptic target genes and neuronal activity-dependent polyadenylation site selection. Neuron *60*, 1022–1038.

Frum, R., Busby, S.A., Ramamoorthy, M., Deb, S., Shabanowitz, J., Hunt, D.F., and Deb, S.P. (2007). HDM2-binding partners: interaction with translation elongation factor EF1alpha. J. Proteome Res. *6*, 1410–1417.

Giagtzoglou, N., Ly, C.V., and Bellen, H.J. (2009). Cell adhesion, the backbone of the synapse: "vertebrate" and "invertebrate" perspectives. Cold Spring Harb. Perspect. Biol. *1*, a003079.

Haas, K.F., Miller, S.L., Friedman, D.B., and Broadie, K. (2007). The ubiquitin-proteasome system postsynaptically regulates glutamatergic synaptic function. Mol. Cell. Neurosci. *35*, 64–75.

Hirano, S., Yan, Q., and Suzuki, S.T. (1999). Expression of a novel protocadherin, OL-protocadherin, in a subset of functional systems of the developing mouse brain. J. Neurosci. *19*, 995–1005.

Keith, D., and El-Husseini, A. (2008). Excitation Control: Balancing PSD-95 Function at the Synapse. Front. Mol. Neurosci. *1*, 4.

Kelleher, R.J., III, and Bear, M.F. (2008). The autistic neuron: troubled translation? Cell *135*, 401–406.

Kim, Y.C., and DeMartino, G.N. (2011). C termini of proteasomal ATPases play nonequivalent roles in cellular assembly of mammalian 26 S proteasome. J. Biol. Chem. *286*, 26652–26666.

Kim, S.Y., Yasuda, S., Tanaka, H., Yamagata, K., and Kim, H. (2011). Non-clustered protocadherin. Cell Adhes. Migr. *5*, 97–105.

McKinsey, T.A., Zhang, C.L., and Olson, E.N. (2002). MEF2: a calcium-dependent regulator of cell division, differentiation and death. Trends Biochem. Sci. *27*, 40–47.

Morishita, H., and Yagi, T. (2007). Protocadherin family: diversity, structure, and function. Curr. Opin. Cell Biol. *19*, 584–592.

Morishita, H., Umitsu, M., Murata, Y., Shibata, N., Udaka, K., Higuchi, Y., Akutsu, H., Yamaguchi, T., Yagi, T., and Ikegami, T. (2006). Structure of the cadherin-related neuronal receptor/protocadherin-alpha first extracellular cadherin domain reveals diversity across cadherin families. J. Biol. Chem. *281*, 33650–33663.

Morrow, E.M., Yoo, S.Y., Flavell, S.W., Kim, T.K., Lin, Y., Hill, R.S., Mukaddes, N.M., Balkhy, S., Gascon, G., Hashmi, A., et al. (2008). Identifying autism loci and genes by tracing recent shared ancestry. Science *321*, 218–223.

Napoli, I., Mercaldo, V., Boyl, P.P., Eleuteri, B., Zalfa, F., De Rubeis, S., Di Marino, D., Mohr, E., Massimi, M., Falconi, M., et al. (2008). The fragile X syndrome protein represses activity-dependent translation through CYFIP1, a new 4E-BP. Cell *134*, 1042–1054.

Niere, F., Wilkerson, J.R., and Huber, K.M. (2012). Evidence for a fragile X mental retardation protein-mediated translational switch in metabotropic glutamate receptor-triggered Arc translation and long-term depression. J. Neurosci. *32*, 5924–5936.

Novara, F., Beri, S., Giorda, R., Ortibus, E., Nageshappa, S., Darra, F., Dalla Bernardina, B., Zuffardi, O., and Van Esch, H. (2010). Refining the phenotype associated with MEF2C haploinsufficiency. Clin. Genet. *78*, 471–477.

Opazo, P., Sainlos, M., and Choquet, D. (2011). Regulation of AMPA receptor surface diffusion by PSD-95 slots. Curr. Opin. Neurobiol. *22*, 453–460.

Pan, F., Aldridge, G.M., Greenough, W.T., and Gan, W.B. (2010). Dendritic spine instability and insensitivity to modulation by sensory experience in a mouse model of fragile X syndrome. Proc. Natl. Acad. Sci. USA *107*, 17768–17773.

Pfeiffer, B.E., Zang, T., Wilkerson, J.R., Taniguchi, M., Maksimova, M.A., Smith, L.N., Cowan, C.W., and Huber, K.M. (2010). Fragile X mental retardation protein is required for synapse elimination by the activity-dependent transcription factor MEF2. Neuron *66*, 191–197.

Pulipparacharuvil, S., Renthal, W., Hale, C.F., Taniguchi, M., Xiao, G., Kumar, A., Russo, S.J., Sikder, D., Dewey, C.M., Davis, M.M., et al. (2008). Cocaine regulates MEF2 to control synaptic and behavioral plasticity. Neuron *59*, 621–633.

Rezvani, K., Teng, Y., Shim, D., and De Biasi, M. (2007). Nicotine regulates multiple synaptic proteins by inhibiting proteasomal activity. J. Neurosci. *27*, 10508–10519.

Sturgill, J.F., Steiner, P., Czervionke, B.L., and Sabatini, B.L. (2009). Distinct domains within PSD-95 mediate synaptic incorporation, stabilization, and activity-dependent trafficking. J. Neurosci. *29*, 12845–12854.

Sung, Y.J., Dolzhanskaya, N., Nolin, S.L., Brown, T., Currie, J.R., and Denman, R.B. (2003). The fragile X mental retardation protein FMRP binds elongation factor 1A mRNA and negatively regulates its translation in vivo. J. Biol. Chem. *278*, 15669–15678.

Tian, X., Kai, L., Hockberger, P.E., Wokosin, D.L., and Surmeier, D.J. (2010). MEF-2 regulates activity-dependent spine loss in striatopallidal medium spiny neurons. Mol. Cell. Neurosci. *44*, 94–108.

Uemura, M., Nakao, S., Suzuki, S.T., Takeichi, M., and Hirano, S. (2007). OL-Protocadherin is essential for growth of striatal axons and thalamocortical projections. Nat. Neurosci. *10*, 1151–1159.

Waung, M.W., Pfeiffer, B.E., Nosyreva, E.D., Ronesi, J.A., and Huber, K.M. (2008). Rapid translation of Arc/Arg3.1 selectively mediates mGluR-dependent LTD through persistent increases in AMPAR endocytosis rate. Neuron *59*, 84–97.

Woods, G.F., Oh, W.C., Boudewyn, L.C., Mikula, S.K., and Zito, K. (2011). Loss of PSD-95 enrichment is not a prerequisite for spine retraction. J. Neurosci. *31*, 12129–12138.

Xu, T., Yu, X., Perlik, A.J., Tobin, W.F., Zweig, J.A., Tennant, K., Jones, T., and Zuo, Y. (2009). Rapid formation and selective stabilization of synapses for enduring motor memories. Nature *462*, 915–919.

Yang, G., Pan, F., and Gan, W.B. (2009). Stably maintained dendritic spines are associated with lifelong memories. Nature *462*, 920–924.

Yasuda, S., Tanaka, H., Sugiura, H., Okamura, K., Sakaguchi, T., Tran, U., Takemiya, T., Mizoguchi, A., Yagita, Y., Sakurai, T., et al. (2007). Activity-induced protocadherin arcadlin regulates dendritic spine number by triggering N-cadherin endocytosis via TAO2beta and p38 MAP kinases. Neuron *56*, 456–471.

Zhang, M., Wang, Q., and Huang, Y. (2007). Fragile X mental retardation protein FMRP and the RNA export factor NXF2 associate with and destabilize Nxf1 mRNA in neuronal cells. Proc. Natl. Acad. Sci. USA *104*, 10057–10062.